# Chapter 6

# PROPERTIES OF $CuInS_2$ FILMS PREPARED USING REPEATED SPRAY PYROLYSIS TECHNIQUE

## 6.1 Introduction

Techniques for making both n- and p-type $CuInS_2$ were discovered several years ago [1]. Since then, a number of papers were published concerning $CuInS_2$ and its potential device applications, particularly as a photovoltaic detector or solar cell [2-4]. Efficiencies of more than 12% have been reached with a Mo/$CuInS_2$/CdS/ZnO cell structure [5]. Deposition of $CuInS_2$ is based on a sequential process using d.c magnetron sputtering of the metals and sulfurization in elemental sulfur vapor, and $CuInS_2$ layer thickness was 3 μm. Scheer et al reported 10.2% efficiency solar cell which also was having 3 μm thick $CuInS_2$ layer [6]. For $CuInS_2$ based solar cell using a Cd-free buffer layer (11.4% efficiency) also the thickness was maintained in the same order [7]. Chemically etched $CuInS_2$ absorber layer with 4 μm thickness yielded an efficiency of 12% as reported by Onuma et al [8]. A four layer structure of solar cell of low ρ- $CuInS_2$/high ρ- $CuInS_2$/high ρ- CdS/low ρ- CdS has been fabricated by Park et al in order to form back surface field and internal electric field by graded band gap [9]. The thickness of the low resistive $CuInS_2$ film was about 1.5 μm and that of high resistivity layer was 0.2 μm so that the total layer thickness is 1.7 μm. They obtained an efficiency of 8.25%. Thick absorber layer naturally improves light absorption and hence photogenerated carriers in the layer.

One of the difficulties in using CSP technique is in the preparation of thick (>1 μm) films by spraying large volumes of solution in a single stretch. It was observed that when large volumes of the solution (say 600 ml) was sprayed in a single stretch, it always resulted in the formation of $CuInS_2$ film with a lot of pinholes resulting in the wastage of large number of samples. But in spite of this difficulty there are certain advantages in using this technique for film preparation. As stated

earlier it is rather easy to vary stoichiometry of samples when prepared using CSP. This is very useful in the case of $CuInS_2$. For example by varying Cu/In and/or S/Cu ratio we could adjust carrier concentration, photosensitivity and also crystallinity. This is important for solar cell fabrication. Moreover this same technique could be used for the deposition of lower electrode (transparent conducting oxide), absorber layer and buffer layer without any break. This is quite useful for large-scale production of solar cells. We tried to modify the technique for the preparation of thick $CuInS_2$. Hence a trial was made to prepare the film by 'repeated spraying' of small quantities of solution and this resulted in improving the thickness of the film without pinholes. Nobody earlier tried this 'multiple spray technique' to increase CIS thickness. Structural, compositional, optical and electrical characterizations were done for films prepared in this way (with different Cu/In molar ratio in spray solution) and the results are presented in this chapter. This was purposefully done to see the variation in photosensitivity with the change in Cu/In ratio. This is important for cell fabrication, as we are varying mainly the majority carrier concentration by changing Cu/In ratio.

## 6.2 Experimental Details

$CuInS_2$ thin films were deposited onto glass substrates from aqueous solutions of $CuCl_2$, $InCl_3$ and thiourea ($CS(NH_2)_2$) by means of CSP technique using compressed air as carrier gas. Equal volumes of the solutions were mixed in appropriate molar concentrations to get different Cu/In ratios. Cu/In ratio was varied from 0.5 to 1.5 keeping S/Cu ratio at 5. Here the molarity of $CuCl_2$ was fixed at 0.025 M, that of thiourea at 0.125 M and the molarity of $InCl_3$ was varied to get different Cu/In ratios. 225 ml of the solution was sprayed onto the glass substrates kept at 300°C. The samples were kept at the same temperature for half an hour after each spray, and then the temperature was reduced to room temperature. The process was repeated four times and thus the total volume of the solution sprayed was 900 ml. Spray rate was kept at 20 ml/min for all cases. Samples were found to be uniform

without any pinholes and were named CIS1, CIS2 and CIS3 having Cu/In ratio 0.5, 1 and 1.5 respectively with S/Cu ratio fixed at 5.

## 6. 3 Results and Discussion

### *6.3.1 Structural Analysis*

XRD pattern of the films deposited with different Cu/In ratio are given in Fig.6.1. The *d* values coincided with that of $CuInS_2$ (JCPDS-270159) with preferential orientation along (112) plane at $2\theta = 27.75^0$. For Cu deficient CIS1 sample, peak at $33.4^0$ corresponds to (220) plane of $\beta$-$In_2S_3$ [10]. There was no such impurity phase for CIS2 and CIS3 samples. Crystallinity of the film improved on increasing the Cu/In ratio. The grain size of the film was calculated from Debye - Scherrer formula. Variation of grain size with Cu/In ratio is given in Table 6.1. Grain size of the films increased with increase in Cu/In ratio. Lattice parameters were calculated to be a = b = 5.55 Å and c = 11.55 Å which was in good agreement with the standard values of a = b = 5.523 Å and c = 11.141 Å. The thickness of the films was found to be 1.17 μm using Stylus method [Fig.6.2].

Table 6.1 Variation of grain size with Cu/In ratio

| Sample | Grain Size (nm) |
|---|---|
| CIS1 | 7.85 |
| CIS2 | 11.69 |
| CIS3 | 24.36 |

Lattice strain was calculated from the plot of $\beta$ Cos$\theta$ versus 4 Sin$\theta$ graph, where $\beta$ represents FWHM. The value was found to decrease from 1.32 to 0.168 for sample CIS1 to sample CIS3. Thus it was clear that as the sample became more stoichiometric, lattice strain decreased considerably.

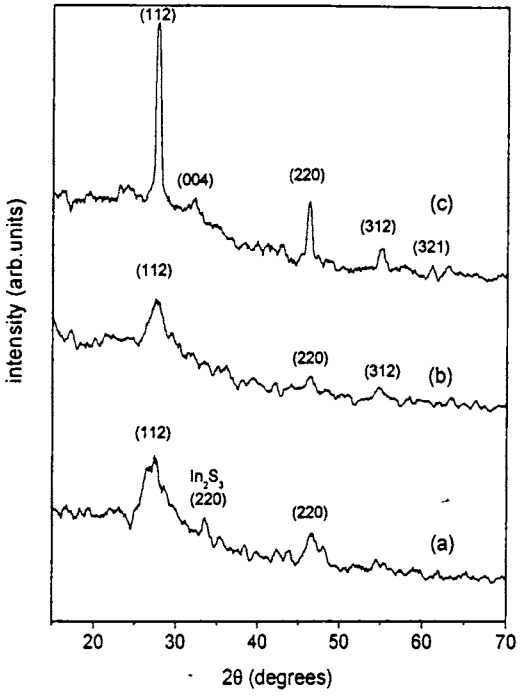


Fig. 6.1XRD pattern: (a) CIS1 (b) CIS2 (c) CIS3

### *6.3.2 Surface Morphology*

Analysis of surface topography using SEM was done on the samples. Surface was not dense and grains were not uniform for Cu- poor films. SEM micrographs showed some agglomerated areas on increasing Cu concentration and surface was denser compared to Cu-poor films. In all cases the surface was found to be rough. SEM micrographs of samples CIS1, CIS2 and CIS3 are given in Fig. 6.3 (a), (b) and (c).

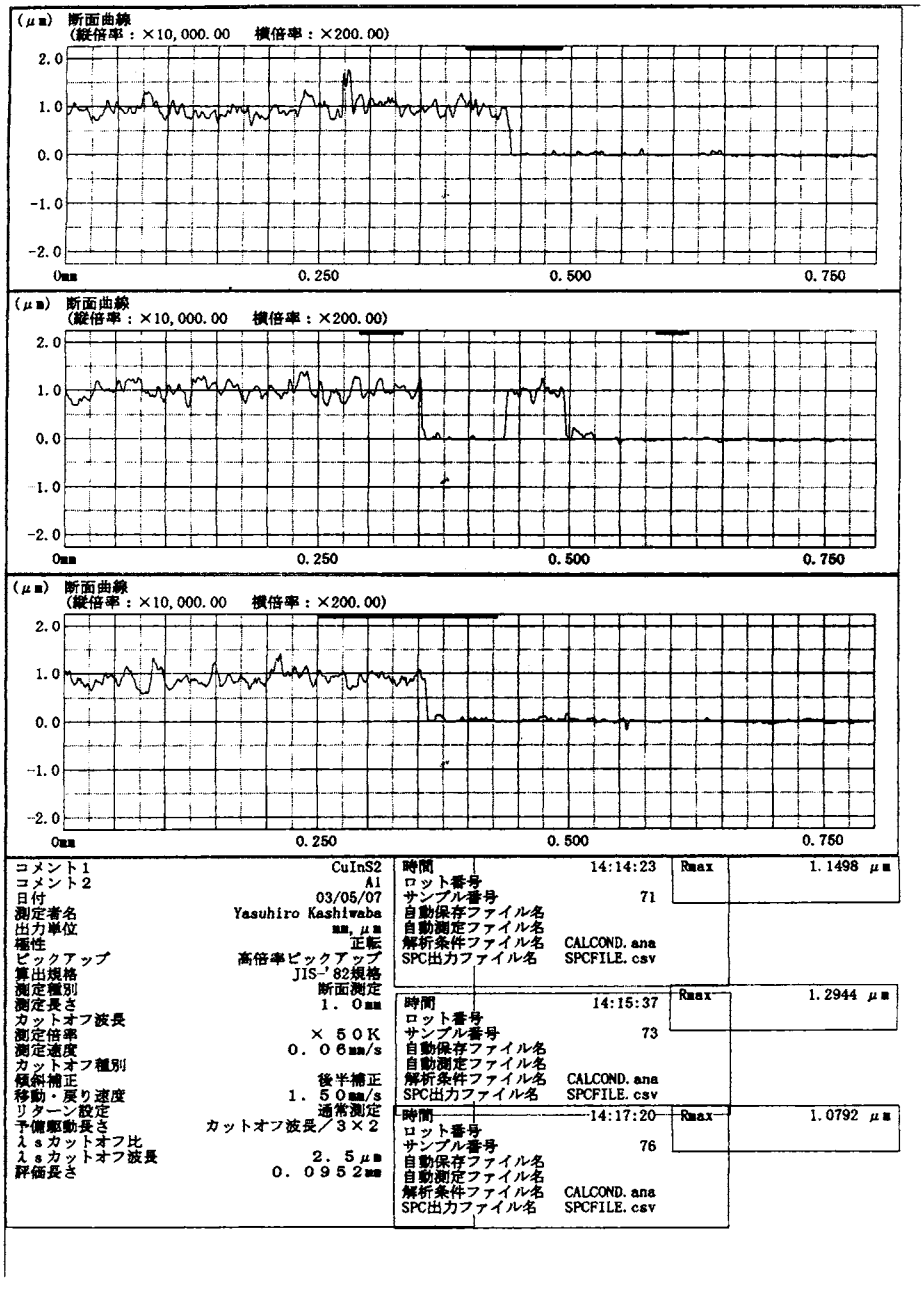


Fig. 6.2 Stylus measurement of $CuInS_2$ film

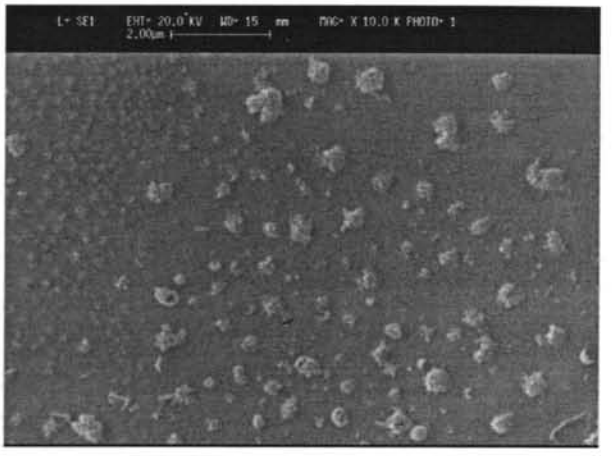
L+ SE1 EHT= 20.0 KV WD= 15 mm MAG= X 10.0 K PHOTO= 1
2.00µm

(a)

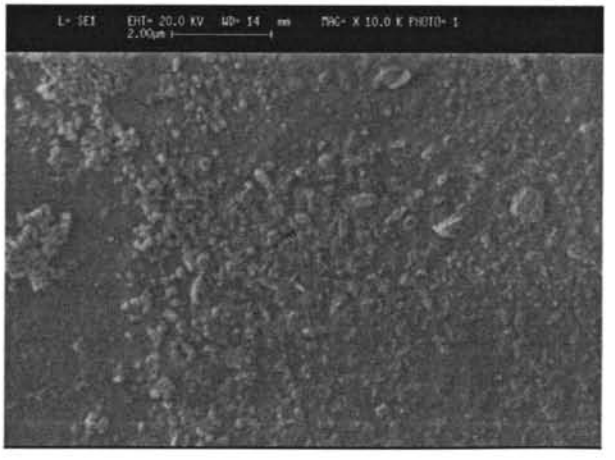
L+ SE1 EHT= 20.0 KV WD= 14 mm MAG= X 10.0 K PHOTO= 1
2.00µm

(b)

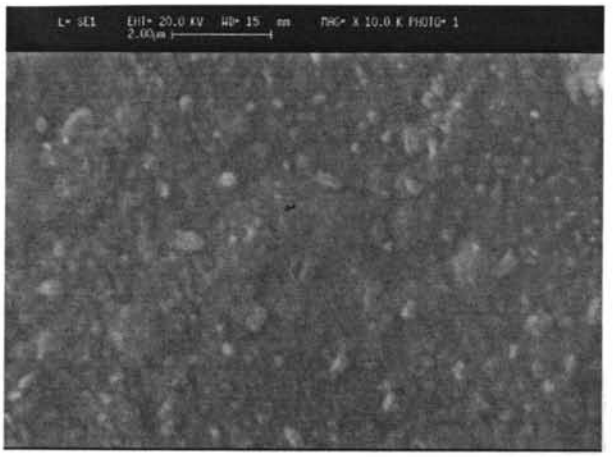

(c)

Fig. 6.3 Scanning Electron Micrograph of
(a) CIS1 (b) CIS2 (c) CIS3 samples

### *6.3.3 EDAX Measurements*

Atomic concentration of Cu, In and S in samples CIS1, CIS2 and CIS3 obtained from EDAX measurements are given in Table 6.2. It had been seen that the Cu/In ratio in the film was always less than that taken in the solution.

Table 6.2 Atomic concentrations from EDAX measurements

| Samples | Cu (%) | In (%) | S (%) | Cu/In ratio in film |
|---|---|---|---|---|
| CIS1 (Cu/In=0.5) | 11.56 | 34.45 | 53.99 | 0.34 |
| CIS2 (Cu/In=1) | 17.95 | 26.69 | 55.36 | 0.67 |
| CIS3 (Cu/In=1.5) | 23.21 | 20.63 | 56.16 | 1.12 |

### *6.3.4 XPS Analysis*

XPS depth profile of the sample CIS2 is given in Fig. 6.4. Binding Energies (BE) of copper, indium and sulfur indicated the formation of $CuInS_2$ [11]. BE values are given in Table 6.3.

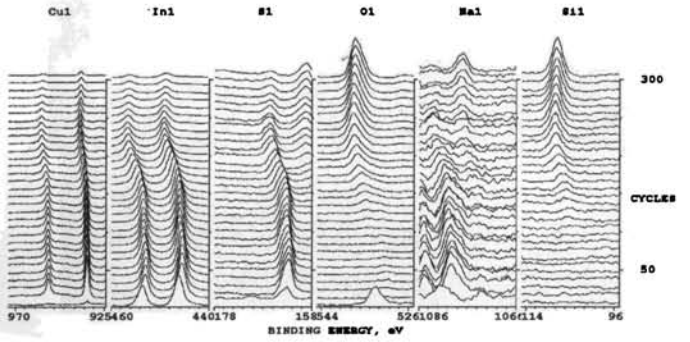


Fig. 6.4 XPS depth profile of CIS2

Table 6.3 BE values of Cu, In and S as observed from XPS analysis

| Element | Binding Energy (eV) |
|---|---|
| $Cu2p_{3/2}$ | 932.7 |
| $Cu2p_{1/2}$ | 952.7 |
| $In3d_{5/2}$ | 445.1 |
| $In3d_{3/2}$ | 452.5 |
| S2p | 162.5 |

It had been found that there was a small quantity of oxygen in the sample near the substrate-film interface, which caused BE shift for copper, indium and sulfur

in that area (after 160 cycles of etching). Multiple heating might have caused $O_2$ diffusing out of glass. However there was no shift in the BE value in the bulk of the sample where there was no oxygen. BE of oxygen (532.5 eV) at the surface indicated surface contamination in the form of sulfate and this was only for ~750 Å (ten cycles) thickness of the film (Binding energy of free oxygen is 531 eV). Decrease in the peak height of sulfur at the surface of the film indicated that this oxygen substituted sulfur in the top layer. But it should be noted that oxygen was not present in the bulk of the sample even after successive heating. But sodium was present throughout the depth of the sample, which might have diffused from the glass substrate, associated with sodium silicate, as there was no sodium content in any of the chemicals used for sample preparation. Decrease in the peak height of Na in glass near film interface proved this. Enhancement in conductivity, crystalline quality and device performance due to incorporation of Na in $CuInS_2$ had been reported [12].

### *6.3.5 Optical Studies*

To determine energy band gap, $(\alpha h\nu)^2$ vs $h\nu$ graph was drawn for all the samples and is represented in Fig.6.5 (a) and (b). It was found that $E_g$ value decreased with increase in Cu/In ratio, from 1.49 eV of sample CIS1 to 1.31 eV of sample CIS3 [13]. This was in accordance with the improvement in crystallinity of the samples with increase in Cu/In ratio [Fig. 6.1].

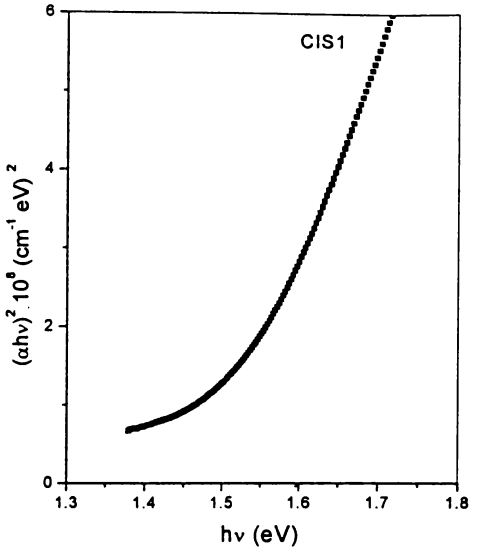


(a)

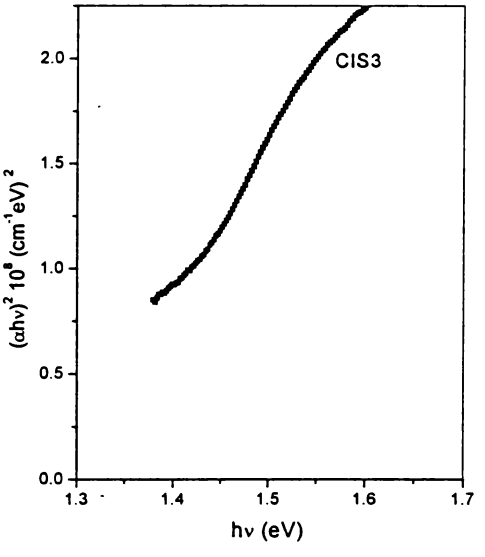


(b)

Fig.6.5 Energy band gap of samples (a) CIS1 (b) CIS3

### *6.3.6 Resistivity and Photosensitivity*

Photosensitivity ($I_L$-$I_D$/$I_D$, where $I_L$ is the current when the sample is illuminated with light and $I_D$ is the dark current) of the samples was also found to decrease with increase in Cu/In ratio. Variation in photosensitivity is shown in Fig.6.6. As Cu/In ratio increased crystallinity of the sample was improved [Fig. 6.1] leading to increase in dark conductivity. Correspondingly number of majority carriers increased and hence the minority carriers surviving to contribute to photosensitivity decreased resulting in reduced photoresponse.

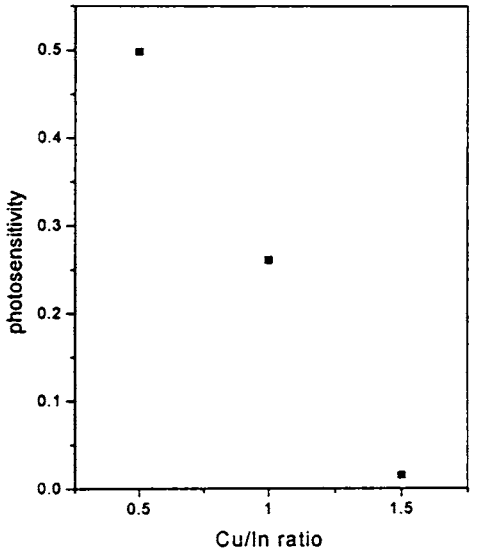


Fig.6.6 Variation in photosensitivity with Cu/In ratio

Resistivity of the samples decreased with increase in Cu/In value. Very high resistivity of samples with excess of indium (Cu/In<1) could be explained by the poor crystallinity (XRD) and due to the reduction in majority carriers caused by the low value of Cu/In ratio. Films with excess copper (Cu/In>1), showed good crystallinity. Here majority carrier concentration also increased with increase in the concentration

of copper and hence increase in conductivity. Resistivity values are compared in Table 6.4.

Table 6.4 Variation of resistivity (ρ) with Cu/In ratio

| Sample | ρ (ohm-cm) |
|---|---|
| CIS1 | $7.56 \times 10^{3}$ |
| CIS2 | $6.36 \times 10^{3}$ |
| CIS3 | $1.13 \times 10^{-1}$ |

### *6.3.7 Temperature Dependent Conductivity Measurements*

Temperature dependence of conductivity (from 100 K) of the samples was measured using computerized setup (IMS 2000, Lab Equip). Measurements at still lower temperatures (from 10 K) were done using liquid helium cryostat having autotuning temperature controller (Lakeshore 321 model). Current and voltage were measured using source measure unit (SMU) (Model: Keithley 236) interfaced by GPIB card and ICS software. Electrical contacts were given using silver paste, painted on surface of the sample at a separation of 0.5 cm.

Figure 6.7 (a), (b) and (c) represent temperature dependent conductivity of samples CIS1, CIS2 and CIS3. It could be seen that the conductivity of CIS3 was much higher than that of CIS1 and CIS2. Conductivity of CIS3 increased steadily from low temperature (100 K) itself unlike the other two samples.

Using Hot Probe, we found that sample CIS1 showed fluctuating nature between *n* and *p* while CIS2 and CIS3 showed clearly p-type conductivity. Arrhenius plot of conductivity of the samples are given in Fig.6.8. Enhanced conduction of CIS2 and CIS3 is apparent from the upward shift of the Arrhenius plots.

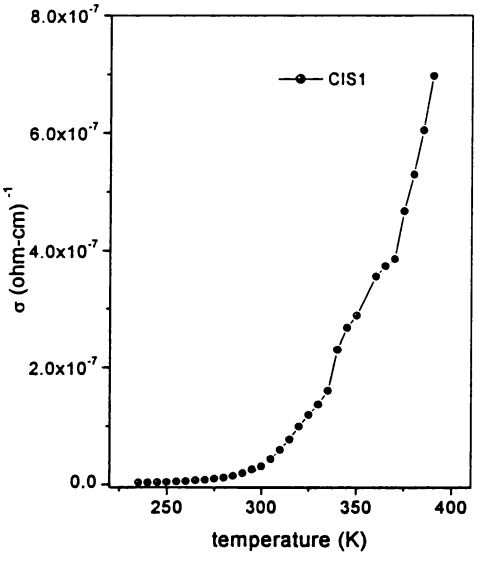
8.0x10⁻⁷
6.0x10⁻⁷
4.0x10⁻⁷
2.0x10⁻⁷
0.0
σ (ohm-cm)⁻¹
CIS1
250
300
350
400
temperature (K)

(a)

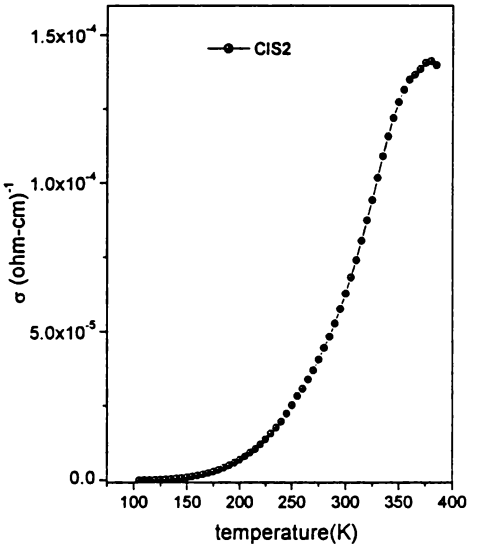
1.5x10⁻⁴
1.0x10⁻⁴
5.0x10⁻⁵
0.0
σ (ohm-cm)⁻¹
CIS2
100
150
200
250
300
350
400
temperature(K)

(b)

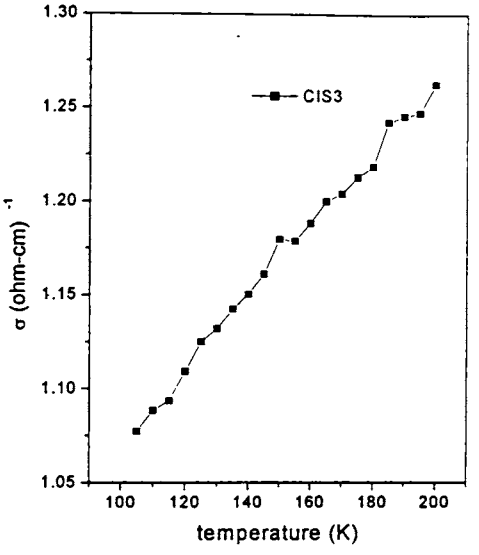


(c)

Fig. 6.7 Temperature dependent conductivity of samples (a) CIS1 (b) CIS2 (c) CIS3

Sample CIS1 indicated two distinct slopes from which activation energies ($E_a$) were calculated as 390 meV and 196 meV. The plots of CIS2 and CIS3 indicated only one slope whose $E_a$ values were 90 meV and 3 meV respectively. Cu deficient $CuInS_2$ (CIS1) had a deep level at 390 meV, which may be another reason for the decrease in conductivity of the sample. This may be acting as majority carrier trap for the sample as described by Kneisel et al [14]. The activation energy of 196 meV correspond to interstitial In ($In_i$) or $In_{Cu}$ [15, 16]. Presence of indium at the interstitial site ($In_i$) or at the Cu vacancy ($In_{Cu}$) might be the reason for the fluctuating nature of conductivity exhibited by the sample. Vacancy of copper created the 90 meV level for CIS2 sample [17].

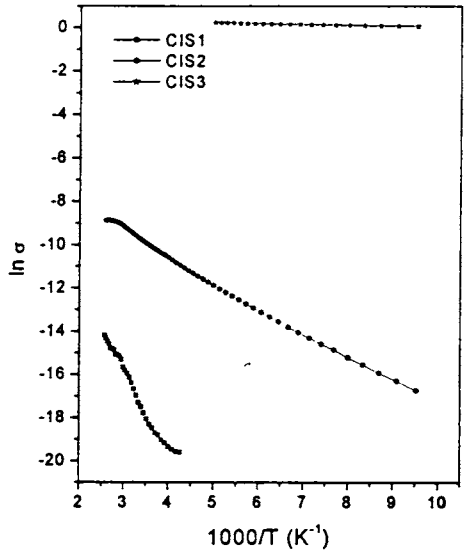


Fig. 6.8 Arrhenius plot of samples CIS1, CIS2 and CIS3

We could find a very shallow level at 3 meV for CIS3 samples, which might be the reason for the high conductivity of the sample. In the first experiment, temperature was varied from 100 K to 200 K using liquid nitrogen cryostat (IMS 2000, Lab Equip). Activation energy was calculated and was found to be 3 meV. Using liquid helium cryostat the temperature was brought down to 10 K and the same experiment was repeated. Even at low temperature the conductivity increased steadily with temperature for CIS3 sample. The result agreed with that of the previous experiment and the activation energy was calculated to be the same. But we could not identify the defect/impurity causing this shallow level in CIS3.

## 6.4 Conclusion

$CuInS_2$ films having thickness of >1 μm could be prepared using multiple spray pyrolysis technique. Greater Cu/In ratio in the solution resulted in larger crystallites and the band gap decreased from 1.49 eV to 1.3 eV. BE values clearly

indicated the formation of $CuInS_2$. Depth profiling of the sample revealed presence of oxygen (only at the film substrate interface) and Na in the sample. The Cu/In ratio in the film was slightly less than that in the solution as observed from EDAX measurements. Temperature dependence of dark conductivity of the samples was also investigated. Two distinct slopes corresponding to activation energies 390 meV (contributing to enhancement of resistivity) and 196 meV ($In_i$ or $In_{Cu}$) were obtained for sample CIS1. Activation energy corresponding to a level of 90 meV ($V_{Cu}$) for CIS2 and 3 meV (contributing to the high conductivity) for CIS3 was also identified. However the reason for the shallow level in CIS3 could not be found out.

## References

[1] B. Tell, J. L. Shay and H. M. Kasper *Phys. Rev. B* **4** (1971) 2463

[2] L. L. Kazmerski, M. S. Ayyagari and G. A. Sanborn *J.Appl.Phys.***46** (1975) 4865

[3] Y. Ogawa, A. J. Waldau, Y. Hashimoto and K. Ito *Jpn. J. Appl. Phys.* **33** (1994) L 1775

[4] S. Uenishi, K. Tohyama and K. Ito *Sol. Energy Mater. Sol. Cells* **35** (1994) 231

[5] J. Klaer, J. Bruns, R. Henninger, K. Siemer, R. Klenk, K. Ellmer and D. Bräunig *Semicond. Sci. Technol.* **13** (1998) 1456

[6] R. Scheer, T. Walter, H. W. Schock, M. L. Fearheiley and H. J. Lewerence *Appl. Phys. Lett.* **63 (24)** (1993) 3294

[7] D. Braunger, D. Hariskos, T. Walter and H. W. Schock *Sol. Energy Mater. Sol. Cells* **40** (1996) 97

[8] Y. Onuma, K. Takeuchi, S. Ichikawa, M. Harada, H. Tanaka, A. Koizumi and Y. Miyajima *Sol. Energy Mater. Sol. Cells* **69** (2001) 261

[9] G. C. Park, H. D. Chung, C. D. Kim, H. R. Park, W. J. Jeong, J. U. Kim, H. B. Gu and K. S. Lee *Sol. Energy Mater. Sol. Cells* **49** (1997) 365

[10] Teny Theresa John, K. C. Wilson, P. M. Ratheesh Kumar, C. Sudha Kartha, K. P. Vijayakumar, Y. Kashiwaba, T. Abe and Y. Yasuhiro *Phys. Stat. Sol. (a)* **202 (1)** (2005) 79

[11] S. Bini, K. Bindu, M. Lakshmi, C. Sudha Kartha, K. P. Vijayakumar, Y. Kashiwaba and T. Abe *Renewable Energy* **20** (2000) 405

[12] T. Watanabe, H. Nakazawa, M. Matsui, H. Ohbo and T. Nakada *Sol. Energy Mater. Sol. Cells* **49** (1997) 357

[13] Teny Theresa John, C. Sudha Kartha , K. P. Vijayakumar, T. Abe and Y. Kashiwaba *Proc. MRSI Theme Symposium*, Varanasi (2004)

[14] J.Kneisel, K. Siemer, I. Luck and D. Bräunig *J. Appl. Phys.* **88 (9)** (2000) 5474

[15] J. H. Schön and E. Bucher *Phys.Stat.Sol. (a)* **171** (1999) 511

[16] P. Lange, H. Neff, M. L. Fearheiley and K. J. Bachmann *J. Electron. Mater.* **14** (1985) 667

[17] J. J. M. Binsma, L. J. Giling and J. Bloem, *J. Lumin.* **27**(1982) 35